SD Stable disease
TS Thymidylate synthase

Introduction

Hepatocellular carcinoma (HCC) is one of the most common malignancies in Asia, including Japan [1, 2], and its prevalence has recently been increasing globally [3]. In most patients, the background of HCC is chronic hepatitis or liver cirrhosis due to hepatitis B or hepatitis C infection. Recently, HCC has increasingly been detected at relatively early stages due to the periodic follow-up of chronic liver disease patients and the development of diagnostic imaging modalities. There have been significant improvements in the treatment of patients with early HCC, and the therapeutic results have been markedly improved by site-specific treatments such as transcatheter arterial chemoembolization, percutaneous ethanol injection therapy, microwave coagulation therapy, and radiofrequency ablation, as well as hepatectomy [4–6].

However, when existing HCC is cured radically, new cancers develop due to the underlying chronic liver disorders. Treatments must then be performed alone or in combination each time a new cancer appears. Repeated treatment often leads to portal vein tumor thrombosis or distant metastasis, making standard treatments difficult to perform. Recently, the treatment efficacy and safety of the molecular targeted drug sorafenib (Nexavar; Bayer HealthCare Pharmaceuticals–Onyx Pharmaceuticals, Leverkusen, Germany) have been reported and the results placed it as a first-line drug [7]. Sorafenib is a small molecule that inhibits tumor-cell proliferation and tumor angiogenesis and increases the rate of apoptosis in a wide range of tumor models. It acts by inhibiting the serine–threonine kinases Raf-1 and B-Raf and the receptor tyrosine kinase activity of vascular endothelial growth factor receptors (VEGFRs) 1, 2, and 3 and platelet-derived growth factor receptor β (PDGFR-β). Llovet et al. [7] reported that sorafenib prolonged median survival and the time to progression by nearly 3 months in about 300 patients with advanced HCC. Although different types of molecular targeted drugs have been under development, there is no treatment option at present for the patients who fail to respond to sorafenib. Thus, second-line treatment for advanced HCC needs to be established.

The oral fluoropyrimidine anticancer drug, S1, includes the dihydropyrimidine dehydrogenase (DPD) inhibitor 5-chloro-2,4-dihydroxypyridine as a component, and this component is expected to exhibit a marked anticancer effect by preventing 5-fluorouracil (5FU) degradation [8–10]. Combination therapy with S-1 and interferon (IFN) has recently been attempted in patients with advanced HCC, and relatively satisfactory results have been reported [11–14]. However, the response rate for this therapy is limited, and the outcome deteriorates in patients resistant to it. Therefore, if the effectiveness of this therapy can be predicted in advance, unnecessary adverse effects can be avoided, and other treatments may be attempted.

We have noted some candidate proteins which may have a possible relationship with the effect of this therapy. The cancer stem-cell marker CD133 [15–18] can reportedly resist anticancer drugs through an intrinsic drug resistance mechanism [19, 20]. Thymidylate synthase (TS) and DPD are enzymes involved in 5FU metabolism, and many reports have suggested their relationship with the therapeutic effects of 5FU in lung [21] and colon cancers [22]. Furthermore, interferon-receptor 2 (IFNR2) is reported to be the most important of the receptors through which IFN acts directly on HCC [23, 24]. Apoptosis is the primary mechanism of the anticancer effect of anticancer drugs, and p53 is closely involved in apoptosis [25–27].

In the present study, we sought to identify factors predicting the effectiveness of S1+ pegylated-interferon (PEG-IFN) α-2b therapy. HCC tissue samples were collected before the therapy was started, the expression levels of CD133, TS, DPD, and IFNR2 proteins were determined by Western blot analysis, and the presence or absence of p53 gene mutations was examined by direct sequencing. We found that the expression level of CD133 was significantly correlated with the therapeutic effect. Thus, measurement of the CD133 expression level before treatment may facilitate prediction of the therapeutic effect and the avoidance of unnecessary adverse effects.

Subjects, materials, and methods

Patients

Between January 2007 and January 2009, a total of 31 patients with refractory HCC that could not be controlled by standard therapeutic modalities (transcatheter arterial chemoembolization, percutaneous ethanol injection therapy, microwave coagulation therapy, radiofrequency ablation, and hepatectomy) underwent S-1 and PEG-IFN α-2b combination therapy. Patient characteristics are shown in Table 1, with more details shown in Table 2. All pathological specimens of HCC were collected by needle biopsy.

Eligibility criteria

Eligibility criteria for the combination therapy included: (1) advanced HCC that was uncontrollable with standard treatment, or HCC with distant metastasis; (2) age <80 years; (3) an Eastern Cooperative Oncology Group performance status of 0 or 1; (4) Child–Pugh grade A; (5) encephalopathy

Table 1 Characteristics of patients treated with combination therapy of S1 and PEG-IFN α-2b

Characteristics	Number of patients
Total	31
Gender	
Male	28
Female	3
Age (years)	
Median	66
Range	30–80
Cause of disease	
HBV	10
HCV	15
Non-HBV, non-HCV	6
Child–Pugh stage	
A	31
BCLC stage	
C (advanced)	31
ECOG performance status	
0	28
1	3

PEG-IFN pegylated interferon, *HBV* hepatitis B virus, *HCV* hepatitis C virus, *BCLC* Barcelona Clinic Liver Cancer Group, *ECOG* Eastern Cooperative Oncology Group

degree 0; (6) leukocyte count >3,000 cells/mm [3]; hemoglobin level >10 g/dl and platelet count >80,000 cells/mm^3; and (7) serum creatinine <1.5 mg/dl, serum aspartate aminotransferase <200 IU/l, serum alanine aminotransferase <200 IU/l, and serum total bilirubin level <3.0 mg/dl. The diagnosis of HCC was made based on the hematoxylin–eosin staining of histopathological specimens in all patients.

Treatment regimen

After the obtaining of informed consent, 31 patients were treated with S-1 (TS1; Taiho Pharmaceutical, Tokyo, Japan) and PEG-IFN α-2b (Pegintron; Schering-Plough, Kenilworth, NJ, USA) combination therapy. S-1 was given orally at a daily dose of 80–120 mg (depending on the body surface area: <1.25 m^2: 80 mg, >1.25 to <1.5 m^2: 100 mg, <1.5 m^2: 120 mg), divided into two equal doses, from days 1 to 28. PEG-IFN α-2b was given subcutaneously at a dose of 50 μg on days 1, 8, 15, and 22. One course consisted of consecutive administration for 28 days followed by a 2-week drug-free interval. The Medical Ethics Committee of Kinki University of Medicine approved the study.

Assessment of response

Responses of HCC patients to the combination therapy were assessed by contrast-enhanced computed tomography after each course. The response was defined according to the Response Evaluation Criteria in Solid Tumours (RECIST). A partial response (PR) was defined as a minimum 30% decrease in the sum of the longest diameters of the target lesions, with the baseline sum of the longest diameters of these lesions as the reference. Progressive disease (PD) was defined as a minimum 20% increase in the sum of the longest diameters of the target lesions. Stable disease (SD) was defined as meeting neither PR nor PD criteria. When the response achieved regarding intrahepatic HCC was different from that for extrahepatic HCC, the poorer one was determined as the achieved response.

Assessment of toxicity

Blood cell counts and biochemical profiles were performed at least once every week. Adverse reactions were assessed using the National Cancer Institute-Common Toxicity Criteria (NCI-CTC, version 3).

Western blot analysis

To prepare tissue lysate, HCC tissue was homogenized with CelLytic-MT Mammalian Tissue Lysis/Extraction reagent (Sigma-Aldrich, St. Louis, MO, USA) along with 2% sodium dodecyl sulfate (SDS) and the protease inhibitor, Complete™ (Roche Diagnostics, Mannheim, Germany), and centrifuged. Equal protein amounts (8 μg) of tissue lysates were electrophoresed through a reducing SDS polyacrylamide gel and electroblotted onto a polyvinylidene difluoride (PVDF) membrane. The membrane was blocked and incubated with polyclonal IgG for TS (1/500; Taiho Pharmaceutical, Tokyo, Japan), DPD (1/3,000; Taiho Pharmaceutical), IFN-α/βR (1/500; Otsuka Pharmaceutical., Tokyo, Japan), CD133 (1/1,000; Cell Signaling Technology, Danvers, MA, USA), and β-actin (1/2,000; Sigma-Aldrich) in Can Get Signal® immunostain solution (TOYOBO, Osaka, Japan). For CD133 detection, lysis of the human colon cancer cells WiDr and DLD1 (positive and negative controls, respectively) was examined. Protein levels were detected using horseradish peroxidase (HRP)-linked secondary antibodies and the ECL-plus System (GE Healthcare, Buckinghamshire, UK).

To evaluate the signal intensity, the obtained Western blot image data were quantified using Image J software (NIH, Bethesda, MD, USA).

Immunohistochemistry

We performed immunohistochemical analysis of paraffin-embedded sections of HCC. Immunohistochemical staining was carried out with antibodies raised against CD133 (1:100), and visualized using the Dako LSAB System-HRP

Table 2 Detailed characteristics and outcomes of patients treated with combination therapy of S1 and PEG-IFN α-2b

Patient no.	Age (years)	Gender	PS	HBs-Ag	HCV-Ab	Type of intrahepatic tumor	Vascular invasion	Metastasis	Tumor grade	Prior treatment	AFP (ng/ml)		DCP (mAU/ml)		Response	Outcome
											Before	After	Before	After		
1	80	M	0	−	−	Nodular	Absence	LN	Poor[a]	OP, TACE	3	3	16	17	PR	21.2 M dead
2	70	M	0	−	−	Nodular	Presence	−	Poor	OP	6	35	5,535	60,413	PD	1.7 M dead
3	66	M	0	−	−	Nodular	Absence	Lung	Moderate[b]	OP, RFA	243	65	74	21	PR	25.4 M alive
4	61	M	0	+	−	Nodular	Absence	LN	Moderate	TACE	474	22	31	13	PR	8.1 M dead
5	62	M	0	+	−	Nodular	Absence	Lung, adrenal	Moderate	OP, HAIC	3,268	1,122	18	21	PD	1.9 M dead
6	67	M	0	+	−	Nodular	Absence	Lung	Moderate	OP, TACE	7,964	8,643	3,124	6,676	PD	1.3 M dead
7	60	M	0	−	+	Nodular	Presence	−	Poor	OP	11	13	19	37	SD	16.7 M alive
8	74	M	1	−	+	Nodular	Absence	−	Poor	OP, TACE	2,242	490	1,147	2,356	PD	3.0 M alive
9	59	F	0	+	−	Nodular	Presence	Lung	Moderate	HAIC	867	536	1,300	413	PR	7.2 M alive
10	70	M	0	−	−	Nodular	Presence	−	Moderate	−	345	26	61,319	1,024	PR	9.2 M alive
11	74	M	0	−	+	Diffuse	Presence	Adrenal	Moderate	HAIC	2,246	1,352	13,303	11,167	PR	6.6 M dead
12	60	M	0	−	+	Diffuse	Presence	−	Moderate	−	51	48	13,007	8,523	PD	3.6 M dead
13	61	M	0	+	−	Nodular	Presence	−	Moderate	−	8	9	476	209	SD	3.8 M alive
14	75	M	0	−	+	Nodular	Absence	LN	Poor	TACE	2,476	11,722	3,711	5,452	NE	0.6 M dead
15	61	M	0	+	−	Nodular	Absence	−	Poor	TACE	251	175	1,470	2,795	PD	3.8 M alive
16	30	M	0	+	−	Nodular	Presence	−	Moderate	−	114,852	79,361	195	183	PR	5.2 M alive
17	80	M	1	−	+	Diffuse	Absence	Lung, LN, bone	Moderate	−	70	106	116,140	306,800	PD	3.2 M dead
18	78	M	1	−	+	Nodular	Presence	Lung	Moderate	−	13,544	10,192	3,401	4,805	PD	2.8 M dead
19	55	M	0	−	+	Nodular	Presence	Lung, LN	Moderate	−	470	468	62,938	31,608	SD	2.0 M dead
20	35	M	0	−	+	Nodular	Presence	−	Moderate	−	91	285	44,951	58,921	PD	2.3 M dead
21	63	M	0	−	+	Nodular	Absence	−	Moderate	OP	1,140	160	412	96	PR	10.2 M alive
22	66	M	0	−	+	Nodular	Absence	−	Poor	TACE	651	872	3,231	5,890	PD	3.1 M dead
23	67	M	0	−	+	Nodular	Absence	Lung	Poor	OP	73	86	16	24	PD	3.1 M dead
24	57	M	0	−	+	Diffuse	Presence	Lung	Moderate	−	154	43	3,891	123	PR	9.5 M alive
25	65	M	0	−	+	Nodular	Absence	Lung	Moderate	OP, TACE	2,118	4,860	45,359	67,894	PD	1.9 M dead
26	51	M	0	+	−	Nodular	Absence	−	Moderate	−	1,111	3,890	240	651	PD	1.9 M dead
27	72	M	0	+	−	Nodular	Presence	Lung	Moderate	TACE	652	612	1,131	980	PD	5.6 M dead
28	74	M	0	+	−	Nodular	Presence	Lung, LN	Moderate	OP, TACE	658	890	2,418	3,168	PD	2.0 M dead
29	75	F	0	−	+	Nodular	Presence	−	Moderate	HAIC	1,153	2,789	11,456	21,998	PD	5.3 M dead
30	68	F	0	−	−	Nodular	Presence	−	Moderate	−	7	7	231	164	PR	16.2 M alive
31	58	M	0	−	−	Nodular	Presence	Lung, adrenal	Poor	TACE	86	58	14,661	11,990	SD	2.0 M alive

PS performance status, *HBs-Ag* hepatitis B surface antigen, *HCV-Ab* anti-hepatitis C virus antibody, *LN* lymph node, *TACE* transcatheter arterial chemoembolization, *RFA* radiofrequency ablation, *HAIC* hepatic arterial infusion chemotherapy using implanted port system, *AFP* alpha-fetoprotein, *DCP* des-gamma-carboxyprothrombin, *OP* operation, *M* months, *PR* partial response, *PD* progressive disease, *SD* stable disease

[a] Poorly differentiated

[b] Moderately differentiated

(Dako, Carpinteria, CA, USA). Sections were counterstained with hematoxylin.

Determination of p53 sequence

Total RNA extracted from HCC tissue using TRIZOL (Invitrogen, Carlsbad, CA, USA) was reverse-transcribed employing the Takara RNA PCR kit (AMV) Ver.3 (Takara, Tokyo, Japan). p53 was amplified using the forward primer 5′-GAGCCGCAGTCAGATCCTA-3′ and the reverse primer 5′-CAGTCTGAGTCAGGCCCTTC-3′, and nested polymerase chain reaction (PCR) was performed using the primers 5′-CCCCTCTGAGTCAGGAAACA-3′ and 5′-TTATGGCGGGAGGTAGACTG-3′. The PCR product was purified and sequenced using BigDye terminator version 3.1 cycle sequencing on an ABI 3100 DNA sequencer (Applied Biosystems, Foster City, CA, USA).

Statistical analysis

Differences between groups were examined for significance using the Mann–Whitney *U*-test and Fishers exact test where appropriate. Multivariate analysis was performed by using a logistic regression model. Cumulative survival and progression-free survival (PFS) curves were constructed using the Kaplan–Meier method and compared using the log-rank test. All the analyses described above were performed using the SPSS program (version 11.5; SPSS, Chicago, IL, USA).

Results

Response

Complete and partial responses were achieved in 0 (0%) and 10 (32.3%) of the 31 patients, respectively. The overall response rate was 32.3%. Stable disease (SD) was noted in 3 patients (9.7%), and the disease control rate (complete response + partial response + SD) was 41.9%. Progressive disease (PD) was noted in 17 patients (54.8%). One patient was excluded from the assessment of response, because the patient died of HCC rupture 17 days after the start of treatment and the computed tomography could not be performed.

Progression-free survival rate and survival assessment

The median PFS was 1.6 months (95% confidence interval [CI] 1.5–1.7 months). The cumulative PFS rates at 6, 12, and 18 months were 38, 19, and 9%, respectively.

All enrolled patients were also included in a survival assessment. Twelve patients were still alive at the end of the observation period (median 8.2 months, range 2–25.4 months), while 19 patients had died. The causes of death were tumor progression ($n = 18$) and infectious lung disease ($n = 1$). The median survival time was 5.3 months (95% CI 1.7–9.0 months). The cumulative survival rates at 6, 12, 18, and 24 months were 44, 35, 35, and 17%, respectively.

Relationship of CD133, TS, DPD, and IFNR2 protein expression levels in HCC with the anticancer effect of the combined therapy

The expression levels of CD133, TS, DPD, and IFNR2 proteins, which were candidate predictive factors for the therapeutic effect, were studied by Western blotting in all specimens. Figure 1 shows the results in five samples from the PR group and four samples from the PD group. The expression level of CD133 was low in the PR group but high in the PD group. However, no marked differences were noted in the expression levels of TS, DPD, or IFNR2 between the two groups.

Next, the relationships of the CD133, TS, DPD, and IFNR2 protein expression levels with the antitumor effect were evaluated. To compare the protein expression levels among specimens, the relative expression level was calculated by dividing the intensity of each signal on Western blotting by the signal intensity of actin, which is an internal control. The CD133 protein expression level was significantly lower in the responder group (median 0.05) than in the nonresponder group (median 0.58) group ($p = 0.005$) (Fig. 2a). In contrast, the TS, DPD, and IFNR2 protein expression levels showed no significant differences between the responder and nonresponder groups (Fig. 2b–d).

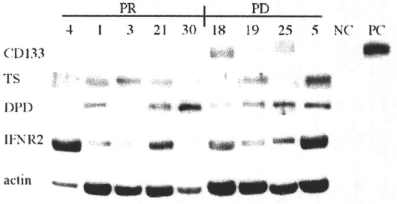

Fig. 1 Expression of CD133, thymidylate synthase (*TS*), dihydropyrimidine dehydrogenase (*DPD*), and interferon receptor 2 (*IFNR2*) as possible factors predicting the therapeutic effect in hepatocellular carcinoma (HCC). Results of Western blotting in typical cases in the partial response (*PR*) and progressive disease (*PD*) groups. For CD133, negative (DLD1) and positive (WiDr) controls were used

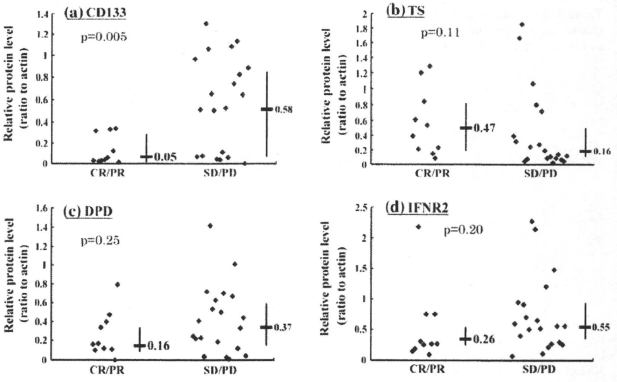

Fig. 2 Relationships between the expression levels of CD133 (**a**), TS (**b**), DPD (**c**), and IFNR2 (**d**) and the anticancer effect. *Vertical lines* on the right of these figures represent the quartile positions, and *horizontal lines* indicate the medians. The numbers of subjects with complete response (*CR*)/PR and stable disease (*SD*)/PD were ten and twenty, respectively

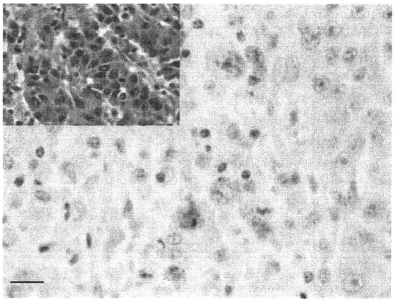

Fig. 3 Immunohistochemistry of CD133 in HCC tissue. This typical sample was intensely positive for CD133. Detection was facilitated using diaminobenzidine (DAB), which shows brown staining when positive. Magnification ×400. *Inset* image is H&E-stained specimen (magnification ×200)

The expression of CD133 was also studied in liver cancer tissues of all specimens using immunohistochemistry. Figure 3 presents specimens that showed intense staining for CD133. The presence or absence of an immunohistological signal was correlated with the CD133 protein expression level determined by Western blotting.

Comparison of the patient background and candidate factors predicting treatment effects with the final outcome (results of univariate analysis and multivariate analysis with a logistic regression model)

Univariate analysis showed a significantly higher CD133 level ($p < 0.01$) in the nonresponder (NR) than the responder group and a slightly higher TS level ($p = 0.11$) in the responder group (Table 3). Using CD133 and TS showing $p < 0.15$ on univariate analysis, multivariate analysis with a logistic regression model was performed. This analysis revealed that only CD133 was a significant factor (odds ratio 0.076, 95% CI 0.007–0.88, $p = 0.039$) (Table 4). Thus, irrespective of the TS level, CD133 was identified as an independent factor predicting the treatment effects.

Relationships of the CD133 protein expression level with the anticancer effect, PFS, and OS

The positive predictive value for nonresponders was 100% in patients whose CD133 expression level exceeded 0.4. Thus, we classified patients into high- and low-CD133 expression groups with a cutoff level of 0.4 (Fig. 2a). Thirteen patients were classified into the high-CD133 expression group and 18 patients into the low-CD133 expression group.

The relationship between the CD133 protein expression level and PFS is shown in Fig. 4. The median PFS was 1.6 months (95% CI 1.5–1.6 months) in the high-CD133 expression group and 7.2 months (95% CI 2–12.3 months) in the low-CD133 expression group. The log-rank test using the Kaplan–Meier method showed that the PFS was significantly prolonged in the low-level compared to the high-level CD133 expression group ($p = 0.036$).

The relationship between the CD133 protein expression level and overall survival (OS) is shown in Fig. 5. The median survival time was 3.1 months (95% CI 1.4–4.8 months) in the high-CD133 expression group, but 8.1 months (95% CI 0–19.3 months) in the low-CD133 expression group. The log-rank test using the Kaplan–Meier

Table 3 Comparison of patient characteristics according to the anticancer effect of the therapy

Variable	Responders (PR) ($n = 10$)	Nonresponders (SD + PD) ($n = 20$)	p value
Age (years)	64.5 (30–80)	65.5 (35–80)	0.85
Sex, no. (%)			0.25
Male	8 (80)	19 (95)	
Female	2 (20)	1 (5)	
Cause of disease, no. (%)			0.21
Hepatitis B	3 (30)	7 (35)	
Hepatitis C	3 (30)	11 (55)	
Non-B, non-C	4 (40)	2 (10)	
ECOG performance status, no. (%)			0.53
0	10 (100)	17 (85)	
1	0 (0)	3 (15)	
Tumor grade, no. (%)			0.21
Moderate	9 (90)	13 (65)	
Poor	1 (10)	7 (35)	
Vascular invasion, no. (%)	6 (60)	11 (55)	1
AFP (ng/ml), median (range)	409.5 (3–114,852)	560.5 (6–13,544)	1
PIVKA II (mAU/ml), median (range)	321.5 (16–61,319)	3,177.5 (16–116,140)	0.17
Previous therapy (last), no. (%)			0.83
OP	2 (20)	4 (20)	
TACE	2 (20)	7 (35)	
HAIC	2 (20)	2 (10)	
None	4 (40)	7 (35)	
CD133, median (range)	0.05 (0.01–0.34)	0.58 (0–1.30)	**<0.01**
IFNR2, median (range)	0.26 (0.09–2.19)	0.55 (0.06–2.27)	0.2
TS, median (range)	0.47 (0.08–1.29)	0.16 (0.03–1.85)	**0.11**
DPD, median (range)	0.16 (0–0.79)	0.37 (0–1.42)	0.25
p53 mutation, no. (%)	1 (10)	2 (10)	1

Values in bold are statistically significant

PR partial response, *SD* stable disease, *PD* progressive disease, *ECOG* Eastern Cooperative Oncology Group, *AFP* alpha-fetoprotein, *TACE* transcatheter arterial chemoembolization, *HAIC* hepatic arterial infusion chemotherapy using implanted port system, *IFNR2* interferon-receptor 2, *TS* thymidylate synthase, *DPD* dihydropyrimidine dehydrogenase, *PIVKA II* protein induced by vitamin K antagonist II

Table 4 Multivariate analysis with a logistic regression model

	Odds ratio	95% CI	p value
CD133 > 0.34	0.076	0.007–0.88	0.039
TS > 0.2	1.643	0.189–14.29	0.653

Cutoff value for each factor was determined by receiver operating characteristic curve (ROC) analysis

CI confidence interval

method showed that, in the low-level CD133 expression group, the OS was significantly prolonged compared to that in the high-level group ($p = 0.022$).

Relationship between p53 mutations and the anticancer effect

Mutant p53 was observed in 3 of the 31 patients. The response rate was 32.1% in the wild-type and 33.3% in the mutant specimens, with no significant difference. The disease control rate was 39.3% in the wild-type and 66.7% in the mutant specimens, with no significant difference.

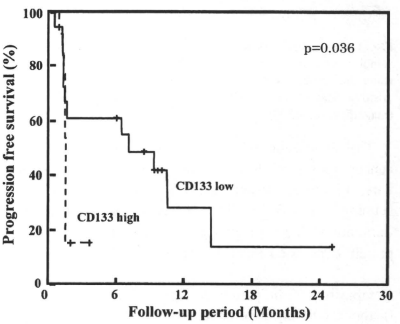

Fig. 4 Progression-free survival of patients who received combination therapy with S-1 and pegylated interferon (PEG-IFN) α-2b, stratified according to the CD133 expression level. Patients were divided into high- and low-CD133 expression groups, with a cutoff value of 0.4 (Fig. 2a). Thirteen and 18 patients belonged to the high- and low-expression groups, respectively

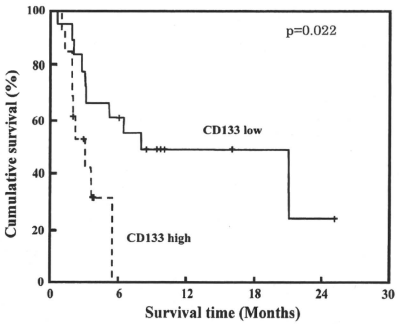

Fig. 5 Kaplan–Meier curve of overall survival in patients treated with combination therapy of S-1 and PEG-IFN α-2b, stratified according to the CD133 expression level

Toxicity

NCI-CTC grade 3 leukocytopenia, neutropenia, anemia, and thrombocytopenia were observed in 2 (6%), 2 (6%), 1 (3%), and 3 (10%) of the 31 patients, respectively. Grade 3 anorexia, stomatitis, rash, and fatigue were observed in 1 (3%), 1 (3%), 1 (3%), and 2 (6%) of the 31 patients, respectively. All adverse effects were alleviated when the treatment was discontinued, leading to no cases of mortality.

Discussion

Here we sought to identify factors predicting the therapeutic effect of S1+ PEG-IFN α-2b therapy in patients with advanced HCC. We collected pathological samples of HCC from all registered patients and studied proteins considered to be related to the therapeutic effect. The expression level of CD133 was significantly correlated with the therapeutic effect, but the expression levels of TS, DPD, and IFNR2, and the presence or absence of p53 mutations were not.

CD133 is a glycoprotein with five transmembrane regions and is a known blood stem-cell marker [28]. It also reportedly acts as a leukemia [15], brain [16], and colon cancer [17, 18] stem-cell marker. The characteristics of cancer stem cells include an ability to proliferate (self-replication capacity) and to differentiate into several cell types with different functions (multidifferentiation capacity), as well as a tumorigenic capacity, which was verified as tumor reproducibility in an experiment involving tumor implantation in an animal model [29–31]. In HCC, CD133-positive cells reportedly possess each of these cancer stem-cell characteristics. In 2007, Ma et al. [32] showed that 65–95% of cells in multiple HCC cell lines were CD133-positive, and Suetsugu et al. [33] reported that the HCC cell line Huh7 expressed CD133. In addition, Song et al. [34], who evaluated 60 patients with HCC, reported both significantly longer postoperative recurrence-free survival and total survival periods in a group with a low compared to that with a high CD133 level. There have been a few such reports on CD133 as a marker of postoperative recurrence.

In the present study, the CD133 protein expression level was significantly lower in the responder group than that in the nonresponder group. HCC showing high-level CD133 expression was resistant to the combination therapy used in this study. Several studies have suggested that the most cancer stem cells exist in the G_0 phase, and a reduced cell cycle velocity is involved in the drug resistance of cancer stem cells [35]. Furthermore, these cells are resistant to reactive oxygen-induced DNA damage because of their high radical-scavenging activities [36]. Furthermore, the drug resistance mechanism of cancer stem cells may also involve ATP binding cassette (ABC) transporters [16, 37]. The anti-apoptotic factors Akt/PKB and Bcl-2 are also activated in CD133-positive liver cancer cells by 5FU administration [38]. Because the anticancer effect of S1+ PEG-IFN α-2b therapy is primarily derived from apoptosis, the activation of Akt/PKB and Bcl-2 is considered to be directly related to the resistance to this therapy.

TS is a rate-regulating enzyme involved in the synthesis of deoxythymidine monophosphate, which is indispensable for DNA synthesis. Therefore, the anticancer effect of 5FU decreases when the TS expression level in the tumor is high, because the drug cannot sufficiently inhibit the enzyme [39]. In the present study, the TS expression level did not correlate with the therapeutic effect. Oie et al. [40] reported that TS expression was suppressed by IFN administration in all the HCC-derived cell lines they examined. Although we did not evaluate the TS expression level after IFN administration, the absence of a correlation between the TS expression level and the therapeutic effect may have been due to the inhibition of TS by IFN.

DPD is a 5FU-degrading enzyme present primarily in the liver. 5FU efficiency increases with low DPD expression in tumor cells [41]. In our study, no correlation between the DPD expression level and therapeutic effect was noted. This was an expected result, because S1 contains a DPD inhibitor.

IFNR, and particularly IFNR2, is considered to be the most important IFN-binding unit for IFN activity. IFNR2 is reportedly expressed in 61–77% of HCCs [42, 43], and its anticancer effect increases with its level of expression. In our study, IFNR2 expression did not correlate with the therapeutic effect. When multiple HCC cell lines were

treated with IFN-α in vitro, a relationship between IFNR2 expression and the anticancer effect was demonstrated [23]. Therefore, IFNR2 is undoubtedly important in the direct anticancer effect of IFN. However, indirect anticancer effects of IFN, such as the activation of natural killer cells and cytotoxic lymphocytes, must also be considered in regard to in vivo treatment [44–46]. Such indirect actions may be primarily responsible for the anticancer effects of IFN in some patients. Regardless of these findings, the IFNR2 expression level is not considered useful for the prediction of the therapeutic effect.

p53 is a typical tumor suppressor gene that may arrest the cell cycle and induce DNA repair or promote apoptosis, depending on the degree of DNA damage [47]. However, the mutation of p53 at some sites causes loss of its original function, allowing the initiation of tumor growth and acceleration of tumor proliferation [48]. In our study, no correlation was noted between the presence or absence of p53 mutations and the therapeutic effect. This may have been because there were only three patients with mutant p53, or because the mutations occurred at sites that do not affect p53 function.

In conclusion, S1+ PEG-IFN α-2b therapy can be a second-line treatment option for patients with advanced HCC, especially in those that show low CD133 expression. Further evaluation with a prospective randomized trial is necessary to confirm the results of the present study.

Acknowledgments The protocol of this study was approved by the Medical Committee of Kinki University of Medicine.

Conflict of interest None.

References

1. Kobayashi M, Ikeda K, Hosaka T, Sezaki H, Someya T, Akuta N, et al. Natural history of compensated cirrhosis in the Child–Pugh class A compared between 490 patients with hepatitis C and 167 with B virus infections. J Med Virol. 2006;78:459–65.
2. Okuda K, Fujimoto I, Hanai A, Urano Y. Changing incidence of hepatocellular carcinoma in Japan. Cancer Res. 1987;47: 4967–72.
3. Parkin DM, Bray F, Ferlay J, Pisani P. Global cancer statistics, 2002. CA Cancer J Clin. 2005;55:74–108.
4. Poon RT, Fan ST, Lo CM, Liu CL, Wong J. Intrahepatic recurrence after curative resection of hepatocellular carcinoma: long-term results of treatment and prognostic factors. Ann Surg. 1999;229:216–22.
5. Sato M, Watanabe Y, Ueda S, Iseki S, Abe Y, Sato N, et al. Microwave coagulation therapy for hepatocellular carcinoma. Gastroenterology. 1996;110:1507–14.
6. Yamasaki T, Kurokawa F, Shirahashi H, Kusano N, Hironaka K, Okita K. Percutaneous radiofrequency ablation therapy with combined angiography and computed tomography assistance for patients with hepatocellular carcinoma. Cancer. 2001;91:1342–8.
7. Llovet JM, Ricci S, Mazzaferro V, Hilgard P, Gane E, Blanc JF, et al. Sorafenib in advanced hepatocellular carcinoma. N Engl J Med. 2008;359:378–90.
8. Shirasaka T, Nakano K, Takechi T, Satake H, Uchida J, Fujioka A, et al. Antitumor activity of 1 M tegafur-0.4M 5-chloro-2, 4-dihydroxypyridine-1M potassium oxonate (S-1) against human colon carcinoma orthotopically implanted into nude rats. Cancer Res. 1996;56:2602–6.
9. Fukushima M, Satake H, Uchida J, Shimamoto Y, Kato T, Takechi T, et al. Preclinical antitumor efficacy of S-1; a new oral formulation of 5-fluorouracil on human tumor xenografts. Int J Oncol. 1998;13:693–8.
10. Cao S, Lu K, Tóth K, Slocum HK, Shirasaka T, Rustum YM. Persistent induction of apoptosis and suppression of mitosis as the basis for curative therapy with S-1, an oral 5-fluorouracil prodrug in a colorectal tumor model. Clin Cancer Res. 1999;5:267–74.
11. Sakon M, Nagano H, Dono K, Nakamori S, Umeshita K, Yamada A, et al. Combined intraarterial 5-fluorouracil and subcutaneous interferon-alpha therapy for advanced hepatocellular carcinoma with tumor thrombi in the major portal branches. Cancer. 2002;94:435–42.
12. Nakamura M, Nagano H, Marubashi S, Miyamoto A, Takeda Y, Kobayashi S, et al. Pilot study of combination chemotherapy of S-1, a novel oral DPD inhibitor, and interferon-alpha for advanced hepatocellular carcinoma with extrahepatic metastasis. Cancer. 2008;112:1765–71.
13. Ueshima K, Kudo M, Nagai T, Tatsumi C, Ueda T, Takahashi S, et al. Combination therapy with S-1 and pegylated interferon alpha for advanced hepatocellular carcinoma. Oncology. 2008;75:106–13.
14. Uka K, Aikata H, Mori N, Takaki S, Kawakami Y, Azakami T, et al. Combination therapy of oral fluoropyrimidine anticancer drug S-1 and interferon alpha for HCC patients with extrahepatic metastasis. Oncology. 2008;75:8–16.
15. Lapidot T, Sirard C, Vormoor J, Murdoch B, Hoang T, Caceres-Cortes J, et al. A cell initiating human acute myeloid leukaemia after transplantation into SCID mice. Nature. 1994;367:645–8.
16. Singh SK, Hawkins C, Clarke ID, Squire JA, Bayani J, Hide T, et al. Identification of human brain tumour initiating cells. Nature. 2004;432:396–401.
17. O'Brien CA, Pollett A, Gallinger S, Dick JE. A human colon cancer cell capable of initiating tumour growth in immunodeficient mice. Nature. 2007;445:106–10.
18. Ricci-Vitiani L, Lombardi DG, Pilozzi E, Biffoni M, Todaro M, Peschle C, et al. Identification and expansion of human colon-cancer-initiating cells. Nature. 2007;445:111–5.
19. O'Brien SG, Guilhot F, Larson RA, Gathmann I, Baccarani M, Cervantes F, et al. Imatinib compared with interferon and low-dose cytarabine for newly diagnosed chronic-phase chronic myeloid leukemia. N Engl J Med. 2003;13:994–1004.
20. Yasui K, Mihara S, Zhao C, Okamoto H, Saito-Ohara F, Tomida A, et al. Alteration in copy numbers of genes as a mechanism for acquired drug resistance. Cancer Res. 2004;64:1403–10.
21. Shintani Y, Ohta M, Hirabayashi H, Tanaka H, Iuchi K, Nakagawa K, et al. New prognostic indicator for non-small-cell lung cancer, quantitation of thymidylate synthase by real-time reverse transcription polymerase chain reaction. Int J Cancer. 2003;104:790–5.
22. Mcleod HL, Sludden J, Murray GI, Keenan RA, Davidson AI, Park K, et al. Characterization of dihydropyrimidine dehydrogenase in human colorectal tumors. Br J Cancer. 1998;77:461–5.
23. Yano H, Iemura A, Haramaki M, Ogasawara S, Takayama A, Akiba J, et al. Interferon alfa receptor expression and growth inhibition by interferon alfa in human liver cancer cell lines. Hepatology. 1999;29:1708–17.

24. Ota H, Nagano H, Sakon M, Eguchi H, Kondo M, Yamamoto T, et al. Treatment of hepatocellular carcinoma with major portal vein thrombosis by combined therapy with subcutaneous interferon-alpha and intra-arterial 5-fluorouracil; role of type 1 interferon receptor expression. Br J Cancer. 2005;93:557–64.
25. Takaoka A, Hayakawa S, Yanai H, Stoiber D, Negishi H, Kikuchi H, et al. Integration of interferon-alpha/beta signaling to p53 responses in tumour suppression and antiviral defence. Nature. 2003;424:516–23.
26. Hagiwara S, Kudo M, Nakatani T, Sakaguchi Y, Nagashima M, Fukuta N, et al. Combination therapy with PEG-IFN-alpha and 5-FU inhibits HepG2 tumour cell growth in nude mice by apoptosis of p53. Br J Cancer. 2007;97:1532–7.
27. Yamamoto T, Nagano H, Sakon M, Wada H, Eguchi H, Kondo M, et al. Partial contribution of tumor necrosis factor-related apoptosis-inducing ligand (TRAIL)/TRAIL receptor pathway to antitumor effects of interferon-alpha/5-fluorouracil against hepatocellular carcinoma. Clin Cancer Res. 2004;10:7884–95.
28. Miraglia S, Godfrey W, Yin AH, Atkins K, Warnke R, Holden JT, et al. A novel five-transmembrane hematopoietic stem cell antigen: isolation, characterization, and molecular cloning. Blood. 1997;90:5013–21.
29. Dean M, Fojo T, Bates S. Tumour stem cells and drug resistance. Nat Rev Cancer. 2005;5:275–84.
30. Zou GM. Cancer initiating cells or cancer stem cells in the gastrointestinal tract and liver. J Cell Physiol. 2008;217:598–604.
31. Sell S, Leffert HL. Liver cancer stem cells. J Clin Oncol. 2008;26:2800–5.
32. Ma S, Chan KW, Hu L, Lee TK, Wo JY, Ng IO, et al. Identification and characterization of tumorigenic liver cancer stem/progenitor cells. Gastroenterology. 2007;132:2542–56.
33. Suetsugu A, Nagaki M, Aoki H, Motohashi T, Kunisada T, Moriwaki H. Characterization of CD133+ hepatocellular carcinoma cells as cancer stem/progenitor cells. Biochem Biophys Res Commun. 2006;351:820–4.
34. Song W, Li H, Tao K, Li R, Song Z, Zhao Q, et al. Expression and clinical significance of the stem cell marker CD133 in hepatocellular carcinoma. Int J Clin Pract. 2008;62:1212–8.
35. Guzman ML, Swiderski CF, Howard DS, Grimes BA, Rossi RM, Szilvassy SJ, et al. Preferential induction of apoptosis for primary human leukemic stem cells. Proc Natl Acad Sci USA. 2002; 99:16220–5.
36. Diehn M, Cho RW, Lobo NA, Kalisky T, Dorie MJ, Kulp AN, et al. Association of reactive oxygen species levels and radioresistance in cancer stem cells. Nature. 2009;458:780–3.
37. Kawabata S, Oka M, Soda H, Shinozawa K, Nakatomi K, Tsurutani J. Expression and functional analyses of breast cancer resistance protein in lung cancer. Clin Cancer Res. 2003; 9:3052–7.
38. Ma S, Lee TK, Zheng BJ, Chan KW, Guan XY. CD133+ HCC cancer stem cells confer chemoresistance by preferential expression of the Akt/PKB survival pathway. Oncogene. 2008; 27:1749–58.
39. Peters GJ, van der Wilt CL, van Triest B, Codacci-Pisanelli G, Johnston PG, van Groeningen CJ, et al. Thymidylate synthase and drug resistance. Eur J Cancer. 1995;31:1299–305.
40. Oie S, Ono M, Fukushima H, Hosoi F, Yano H, Maruyama Y, et al. Alteration of dihydropyrimidine dehydrogenase expression by IFN-alpha affects the antiproliferative effects of 5-fluorouracil in human hepatocellular carcinoma cells. Mol Cancer Ther. 2007;6:2310–8.
41. Etienne MC, Chéradame S, Fischel JL, Formento P, Dassonville O, Renée N, et al. Response to fluorouracil therapy in cancer patients; the role of tumoral dihydropyrimidine dehydrogenase activity. J Clin Oncol. 1995;13:1663–01670.
42. Takayama A, Yano H, Ogasawara S, Higaki K, Kojiro M. Expression of Hu-IFN-alpha R2 chain of Type 1 interferon receptor in human hepatocellular carcinoma and non-cancerous tissues. Int J Mol Med. 2000;6:621–7.
43. Kondo M, Nagano H, Sakon M, Yamamoto H, Morimoto O, Arai I, et al. Expression of interferon alpha/beta receptor in human hepatocellular carcinoma. Int J Oncol. 2000;17:83–8.
44. Kaido T, Macury C, Gresser I. Host CD4+ T lymphocytes are required for the synergistic action of IFN alpha/beta and adoptively transferred immune cells. Int J Cancer. 1994;57:538–43.
45. Lindahl P, Leary P, Gresser I. Enhancement by interferon of the specific cytotoxicity of sensitized lymphocytes. Proc Natl Acad Sci USA. 1972;69:721–4.
46. Uno K, Shimizu S, Ido M, Naito K, Inaba K, Oku T, et al. Direct and indirect effect of interferon on in vivo murine tumor growth. Cancer Res. 1985;45:1320–7.
47. Levine AJ, Monmand J, Finlay CA. The p53 tumour suppressor gene. Nature. 1991;351:435–56.
48. Symonds H, Krall L, Remington L, Saenz-Robles M, Lowe S, Jacks T, et al. p53-dependent apoptosis suppresses tumor growth and progression in vivo. Cell. 1994;78:703–11.

DOI:10.1158/1535-7163.MCT-10-0544

Preclinical Development

Molecular Cancer Therapeutics

Sorafenib Inhibits the Hepatocyte Growth Factor–Mediated Epithelial Mesenchymal Transition in Hepatocellular Carcinoma

Tomoyuki Nagai[1,2], Tokuzo Arao[1], Kazuyuki Furuta[1], Kazuko Sakai[1], Kanae Kudo[1,2], Hiroyasu Kaneda[1], Daisuke Tamura[1], Keiichi Aomatsu[1], Hideharu Kimura[1], Yoshihiko Fujita[1], Kazuko Matsumoto[1], Nagahiro Saijo[3], Masatoshi Kudo[2], and Kazuto Nishio[1]

Abstract

The epithelial mesenchymal transition (EMT) has emerged as a pivotal event in the development of the invasive and metastatic potentials of cancer progression. Sorafenib, a VEGFR inhibitor with activity against RAF kinase, is active against hepatocellular carcinoma (HCC); however, the possible involvement of sorafenib in the EMT remains unclear. Here, we examined the effect of sorafenib on the EMT. Hepatocyte growth factor (HGF) induced EMT-like morphologic changes and the upregulation of SNAI1 and N-cadherin expression. The downregulation of E-cadherin expression in HepG2 and Huh7 HCC cell lines shows that HGF mediates the EMT in HCC. The knockdown of SNAI1 using siRNA canceled the HGF-mediated morphologic changes and cadherin switching, indicating that SNAI1 is required for the HGF-mediated EMT in HCC. Interestingly, sorafenib and the MEK inhibitor U0126 markedly inhibited the HGF-induced morphologic changes, SNAI1 upregulation, and cadherin switching, whereas the PI3 kinase inhibitor wortmannin did not. Collectively, these findings indicate that sorafenib downregulates SNAI1 expression by inhibiting mitogen-activated protein kinase (MAPK) signaling, thereby inhibiting the EMT in HCC cells. In fact, a wound healing and migration assay revealed that sorafenib completely canceled the HGF-mediated cellular migration in HCC cells. In conclusion, we found that sorafenib exerts a potent inhibitory activity against the EMT by inhibiting MAPK signaling and SNAI1 expression in HCC. Our findings may provide a novel insight into the anti-EMT effect of tyrosine kinase inhibitors in cancer cells. *Mol Cancer Ther; 10(1); 169–77. ©2011 AACR.*

Introduction

Hepatocellular carcinoma (HCC) is the fifth most common cancer and the third largest cause of cancer-related death in the world annually (1). Recurrence, metastasis, and the development of new primary tumors are the most common causes of mortality among patients with HCC (2). Sorafenib (Nexavar; Bayer HealthCare Pharmaceuticals Inc.) is a small molecule that inhibits the kinase activities of Raf-1 and B-Raf in addition to VEGFRs, PDGFR-β (platelet-derived growth factor receptor β), Flt-3, and c-KIT (3). Two recent randomized controlled trials reported a clinical benefit of single-agent sorafenib in extending overall survival in both Western and Asian patients with advanced unresectable HCC (4, 5). The potential action mechanisms that lead to these clinical benefits are thought to include antiangiogenic effects and sorafenib's characteristic inhibitory effect on Raf-1 and B-Raf signaling.

Meanwhile, growing evidence indicates that the epithelial mesenchymal transition (EMT), a developmental process by which epithelial cells reduce intercellular adhesions and acquire fibroblastoid properties, has important roles in the development of the invasive and metastatic potentials of cancer progression (6–8). To date, numerous clinicopathologic studies have shown positive correlations between the expressions of the transcription factors SNAI1 (snail homologue 1/SNAIL) and SNAI2 (snail homologue 2/Slug), which are key inducible factors of the EMT, and poor clinical outcomes in breast, ovary, colorectal, and lung cancer; squamous cell carcinoma; melanoma, and HCC (reviewed in ref. 6).

Generally, the activation of a wide variety of ligands including FGF (fibroblast growth factor), TGF-β–BMPs (bone morphogenetic protein), Wnt, EGF (epidermal growth factor), VEGF, and HGF (hepatocyte growth factor) and its receptor can upregulate the expression of EMT-regulating transcription factors, including SNAI1, SNAI2, ZEB1, ZEB2, and TWIST (6). Among them, HGF (also known as scattering factor) activates

Authors' Affiliations: Departments of [1]Genome Biology, [2]Gastroenterology and [3]Medical Oncology, Kinki University School of Medicine, Japan

Note: Supplementary material for this article is available at Molecular Cancer Therapeutics Online (http://mct.aacrjournals.org/).

Corresponding Author: Kazuto Nishio, Department of Genome Biology, Kinki University School of Medicine, 377-2 Ohno-higashi, Osaka-Sayama, Osaka 589-8511, Japan. Phone: 81-72-366-0221 (ext 3150); Fax: 81-72-367-6369; E-mail: knishio@med.kindai.ac.jp

doi: 10.1158/1535-7163.MCT-10-0544

DOI:10.1158/1535-7163.MCT-10-0544

the Met signaling pathway, thereby increasing the invasive and metastatic potentials of the cells and allowing the survival of cancer cells in the bloodstream in the absence of anchorage (9). In addition, HGF is well known as a potent angiogenic cytokine, and Met signal activation can modify the microenvironment to facilitate cancer progression (9). Therefore, the HGF-Met signaling pathway is regarded as a promising therapeutic target, and many molecular targeted drugs are under clinical development (10). In HCC, the mRNA levels of HGF and Met receptor are markedly increased compared with those in normal liver (11). A high serum HGF concentration is associated with a poor prognosis for overall survival after hepatic resection, and the serum level of HGF represents the degree of the carcinogenic state in the livers of patients with C-viral chronic hepatitis and cirrhosis (12–14). Thus, we examined the effect of sorafenib on the HGF-Met–mediated EMT in HCC.

Materials and Methods

Reagents

Sorafenib was provided by Bayer HealthCare Pharmaceuticals Inc. U0126, wortmannin (Cell Signaling Technology), and human HGF (R&D Systems) were purchased from the indicated companies. The structures of compounds are shown in Supplementary Figure 1.

Cell culture

The human HCC cell lines HepG2 and Huh7 were maintained in Dulbecco's modified Eagle's (DMEM) medium (Sigma) supplemented with 10% FBS, penicillin, and streptomycin (Sigma) in a humidified atmosphere of 5% CO_2 at 37°C. The cell lines were obtained from the Japanese Collection of Research Bioresources and were grown in culture for less than 6 months.

Scratch assay

The method used for the scratches assay has been previously described (15). Briefly, the cells were plated onto 24-well plates and incubated in DMEM containing 10% FBS until they reached subconfluence. Scratches were introduced to the subconfluent cell monolayer, using a plastic pipette tip. The cells were then cultured with DMEM containing 10% FBS at 37°C. After 24 hours, the scratch area was photographed using a light microscope (IX71; Olympus). The wound distance between edge to edge were measured and averaged from 5 points per 1 wound area, using DP manager software (Olympus). The 2 wound areas were evaluated in an experiment and the experiment was done in triplicate.

Migration assay

The migration assays were done using the Boyden chamber methods and polycarbonate membranes with an 8-μm pore size (Chemotaxicell), as previously described (15). The membranes were coated with fibronectin on the outer side and dried for 2 hours at room temperature. The cells to be analyzed (2×10^4 cells/well) were then seeded onto the upper chambers with 200 μL of migrating medium (DMEM containing 0.5% FBS), and the upper chambers were placed into the lower chambers of 24-well culture dishes containing 600 μL of DMEM containing 10% FBS or with 10 ng/mL of HGF or with HGF and 10 μmol/L of sorafenib. After incubation for 36 hours (HepG2) and 24 hours (Huh7), the media in the upper chambers were aspirated and the nonmigrated cells on the inner sides of the membranes were removed using a cotton swab. The cells that had migrated to the outer side of the membranes were fixed with 4% paraformaldehyde for 10 minutes, stained with 0.1% Giemsa stain solution for 15 minutes, and then counted using a light microscope. Migrated cells were averaged from 5 fields per 1 chamber and 3 chambers were used on 1 experiment. The experiment was done in triplicate.

Morphologic analysis

HepG2 and Huh7 cells (2×10^4 and 1×10^4 cells/well, respectively) were seeded in 6-well tissue culture dishes. After 24 hours of incubation, the cells were stimulated with 10 ng/mL of HGF or control PBS. When the inhibitors were used, the cells were exposed to each inhibitor for 3 hours before the addition of HGF. After 48 hours, the cells were analyzed using a light microscope. The experiment was done in triplicate.

Western blot analysis

The following antibodies were used in this study: phospho-Met (Y1349), Met, phospho-AKT (S473), AKT, phospho-p44/42 mitogen-activated protein kinase (MAPK), SNAI1/Snail, E-cadherin, N-cadherin, vimentin, β-actin antibody horseradish peroxidase–conjugated secondary antibody (Cell Signaling Technology), and fibronectin (Santa Cruz Biotechnology). All the experiments were done at least in duplicate. The Western blot analysis was done as described previously (16). The data were quantified by automated densitometry using Multigauge Ver. 3.0 (Fujifilm). Densitometric data were normalized by β-actin in triplicate and the average was shown above the Western blot as a ratio of control sample.

Real-time reverse transcription PCR

The real-time reverse transcription PCR (RT-PCR) method has been previously described (17). Briefly, 1 μg of total RNA from the cultured cells was converted to cDNA using a GeneAmp RNA-PCR kit (Applied Biosystems). Real-time RT-PCR amplification was done using a Thermal Cycler Dice (Takara) in accordance with the manufacturer's instructions under the following conditions: 95°C for 6 minutes, 40 cycles of 95°C for 15 seconds, and 60°C for 1 minute. Glyceraldehyde 3-phosphate dehydrogenase (GAPD) was used to normalize the expression levels in the subsequent quantitative analyses. To amplify the target genes, the following primers were purchased from TaKaRa: *CDH1*, forward 5′-TTA AAC

DOI:10.1158/1535-7163.MCT-10-0544

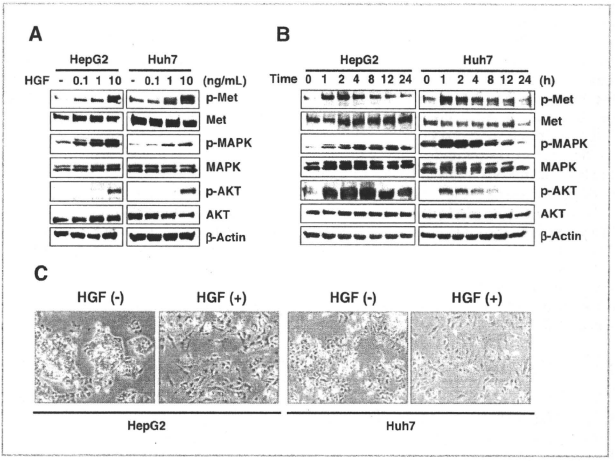

Figure 1. HGF stimulates the Met signaling pathway and induces morphologic changes in HCC. A, HGF stimulation (0, 0.1, 1, and 10 ng/mL) dose-dependently increased the phosphorylation of Met, MAPK, and AKT in the HCC cell lines HepG2 and Huh7. The results of a Western blot analysis are shown. β-Actin was used as a loading control. The serum-starved cells were stimulated with HGF for 60 minutes and then collected for analysis. B, time-course analysis of HGF stimulation. The HCC cells were stimulated with 10 ng/mL of HGF for 0, 1, 2, 4, 8, 12, and 24 hours. The results of a Western blot analysis are shown. C, HGF-mediated morphologic changes included cell scattering and the elongation of the cell shape that are characteristic of the EMT. The HepG2 and Huh7 cells were stimulated with or without 10 ng/mL of HGF for 48 hours and then photographed (magnification × 200).

TCC TGG CCT CAA GCA ATC-3′ and reverse 5′-TCC TAT CTT GGG CAA AGC AAC TG-3′; *CDH2*, forward 5′-CGA ATG GAT GAA AGA CCC ATC C-3′ and reverse 5′-GGA GCC ACT GCC TTC ATA GTC AA-3′; *SNAI1*, forward 5′-TCT AGG CCC TGG CTG CTA CAA-3′ and reverse 5′-ACA TCT GAG TGG GTC TGG AGG TG-3′; *SNAI2*, forward 5′-ATG CAT ATT CGG ACC CAC ACA TTA C-3′ and reverse 5′-AGA TTT GAC CTG TCT GCA AAT GCT C-3′; *VIM*, forward 5′-TGA GTA CCG GAG ACA GGT GCA G-3′ and reverse 5′-TAG CAG CTT CAA CGG CAA AGT TC-3′; *FN1*, forward 5′-GGA GCA AAT GGC ACC GAG ATA-3′ and reverse 5′-GAG CTG CAC ATG TCT TGG GAA C-3′; and *GAPD*, forward 5′-GCA CCG TCA AGG CTG AGA AC-3′ and reverse 5′-ATG GTG GTG AAG ACG CCA GT-3′.

Small interfering RNA transfection

Three different sequences of small interfering RNA (siRNA) targeting human SNAI1 (Hs_SNAI1_9785, 9786, and 9787) and those of 2 scramble control siRNAs were purchased from Sigma Aldrich Japan. The transfection methods have been previously described (17).

Statistical analysis

The statistical analyses were done using Microsoft Excel (Microsoft) both to calculate the SD and to test for statistically significant differences between the samples using a Student *t* test. A value $P < 0.05$ was considered statistically significant.

Results

To examine the activity of HGF-Met signaling in HCC cells, we examined the expressions of phospho-Met, Met, phospho-AKT, AKT, phospho-MAPK, and MAPK in the HepG2 and Huh7 cell lines, using Western blotting. The phosphorylation levels of Met, AKT, and MAPK were dose-dependently increased by HGF stimulation (Fig. 1A). A time-course analysis showed that the phosphorylation levels of Met, AKT, and MAPK peaked at 1 to 2 hours after HGF stimulation and gradually recovered to the baseline values at 4 hours later (Fig. 1B). These results indicated that Met signaling is actually capable of being activated in response to HGF in HCC cells.

From a morphologic aspect, the EMT is characterized by an increase in cell scattering and an elongation of the cell shape (18). To evaluate whether HGF mediates the morphologic change that is characteristic of the EMT in HCC cells, cellular morphology was examined after HGF stimulation. HGF clearly mediated both cell scattering and the elongation of the cell shape in HepG2 and Huh7 cell lines (Fig. 1C). These data indicate that HGF mediates

DOI:10.1158/1535-7163.MCT-10-0544

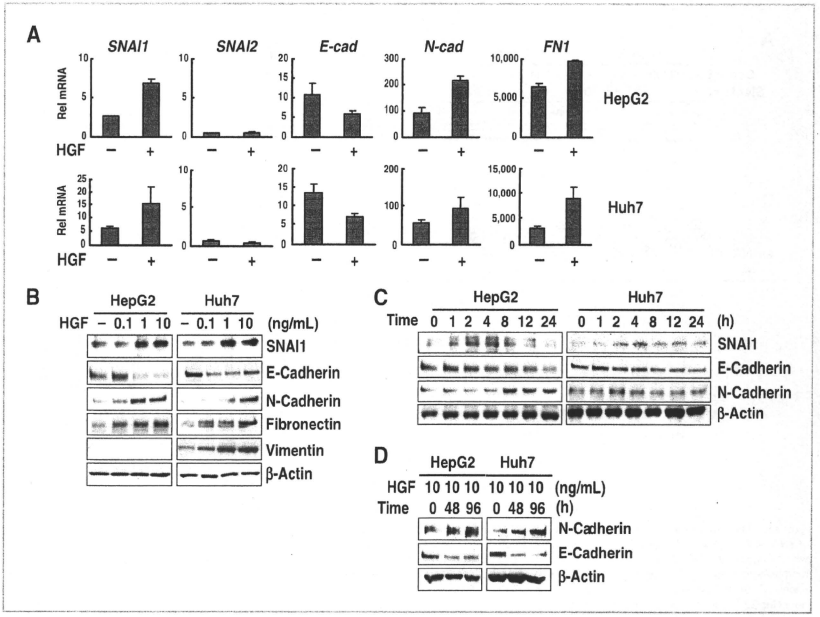

Figure 2. HGF upregulates SNAI1 expression and induces cadherin switching in HCC. A, changes in the mRNA expressions of the EMT-related genes *SNAI1/Snail*, *SNAI2/Slug*, *E-cadherin/CDH1*, *N-cadherin/CDH2*, and *fibronectin/FN1* were determined using real-time RT-PCR. The HepG2 and Huh7 cells were stimulated with or without 10 ng/mL of HGF for 2 hours (SNAI1 and SNAI2) or 48 hours (*E-cad*, *N-cad*, and *FN1*). Rel mRNA, normalized mRNA expression levels (target genes/GAPD $\times 10^4$); E-cad, E-cadherin; N-cad, N-cadherin. B, the HGF-mediated protein expression changes in SNAI1, E-cadherin, N-cadherin, fibronectin, and vimentin were determined using a Western blot analysis. The HepG2 and Huh7 cells were stimulated with HGF at the indicated dose (0, 0.1, 1, or 10 ng/mL) and collected for analysis after 4-hour stimulation for SNAI1 and 72 hours for the others. C, the cells were stimulated with 10 ng/mL of HGF for the indicated time course (0, 1, 2, 4, 8, 12, or 24 hours) and used for analysis. β-Actin was used as a loading control. D, Western blot analysis of E-cadherin and N-cadherin. The cells were stimulated with 10 ng/mL of HGF for 0, 48, and 96 hours and then analyzed.

the morphologic changes that are compatible with the induction of the EMT in HCC cell lines.

Because SNAI1 and SNAI2 are considered to be master regulators of the EMT, changes in the mRNA expression levels of EMT-related genes in response to HGF stimulation were evaluated using real-time RT-PCR (Fig. 2A). HGF stimulation upregulated SNAI1 mRNA expression by more than 2-fold, whereas the baseline expression of SNAI2 was very low compared with that of SNAI1 and did not respond to HGF in either of the HCC cell lines that were examined. Cadherin switching, which is characterized by the downregulation of E-cadherin and the upregulation of N-cadherin, is known as one of the most pivotal cellular events in the EMT (19). Cadherin switching was clearly observed on the basis of mRNA levels after HGF stimulation. The mesenchymal marker fibronectin was also upregulated (Fig. 2A).

Consistent with the mRNA changes, HGF stimulation dose-dependently upregulated the protein expression of SNAI1, N-cadherin, fibronectin, and vimentin and downregulated the expression of E-cadherin in both cell lines (Fig. 2B). Vimentin expression of HepG2 was not detected (baseline vimentin mRNA was also extremely low; data not shown). A time-course analysis showed that HGF upregulated the SNAI1 expression at 2 hours after stimulation and that the expression level recovered to the baseline value at 24 hours thereafter (Fig. 2C). Cadherin switching after HGF stimulation was observed at 8 hours later in HepG2 cells and 48 hours later in Huh7 cells (Fig. 2C and D). Generally, upregulation of SNAI1 is

DOI:10.1158/1535-7163.MCT-10-0544

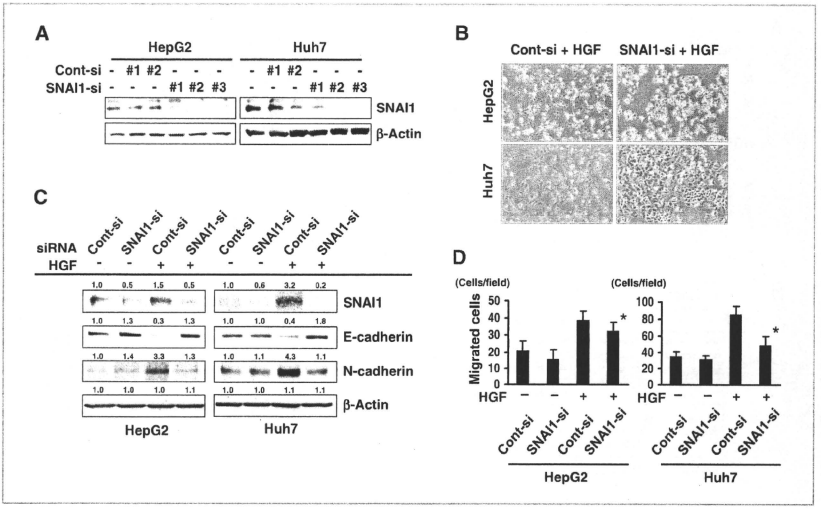

Figure 3. SNAI1 is required to induce the HGF-mediated EMT in HCC cells. A, knockdown of HGF-mediated SNAI1 expression using siRNA. Three sequences of SNAI1-siRNA (1, 2, and 3) were used. The HepG2 and Huh7 cells were treated with or without 50 nmol/L of each siRNA for 48 hours and then were stimulated with 10 ng/mL of HGF. SNAI1-siRNA #2 was effective and was used in subsequent experiments. B, SNAI1 knockdown canceled the HGF-mediated morphologic changes. The HepG2 and Huh7 cells were treated with 50 nmol/L of siRNA for 48 hours and were then stimulated with 10 ng/mL of HGF in all 4 panels. C, SNAI1 suppression by siRNA strongly canceled the HGF-mediated downregulation of E-cadherin and the upregulation of N-cadherin in both HepG2 and Huh7 cells. The cells were treated with 50 nmol/L of siRNA for 48 hours and were analyzed using a Western blot analysis. Densitometric data are shown above the Western blot. D, the siRNA knockdown of SNAI1 inhibited the HGF-mediated cellular migration. The siRNA-transfected HepG2 and Huh7 cells were evaluated using migration assay. The migration assays were conducted using the Boyden chamber methods as described in Materials and Methods. *, $P < 0.05$ (Cont-si vs. SNAI1-si with HGF); Cont-si, control-siRNA; SNAI1-si, SNAI1-targeting siRNA.

observed within few hours, but cadherin switching occurs around 24 hours later after stimulation (20, 21), consistent with our result. These results indicate that HGF meditates the induction of SNAI1, cadherin switching, and the EMT in HCC cells.

Besides SNAI1 and SNAI2, other transcription factors of several genes also have the potential to repress E-cadherin and to induce the EMT; these factors include ZEB1/TCF8, ZEB2/SMAD interacting protein 1, TWIST, E47/TCF3, and TCF4/E2-2 (6). Therefore, we examined whether SNAI1, among several EMT-inducible genes, has a central role in the HGF-mediated EMT in HCC cells. Three sequences of SNAI1-siRNA (1, 2, and 3) were used. A Western blot showed that both sequences 2 and 3 of SNAI1-siRNA completely suppressed the HGF-mediated upregulation of SNAI1 in the HepG2 and Huh7 cells (Fig. 3A); thus, the #2 SNAI1-siRNA was used in the following experiments: The siRNA knockdown of SNAI1 canceled the morphologic changes observed in HepG2 cells undergoing HGF-mediated EMT, whereas the control-siRNA did not (Fig. 3B). Similar results were obtained in Huh7 cells, indicating that SNAI1 is required for the morphologic changes observed in HGF-mediated EMT. Similarly, the siRNA knockdown of SNAI1 strongly canceled the HGF-mediated downregulation of E-cadherin and the upregulation of N-cadherin in both HepG2 and Huh7 cells (Fig. 3C). Those of mRNA expression changes were relatively correlated with the results of Western blot, except for N-cadherin in Huh7 cells (Supplementary Fig. 2A). Regarding the cellular migration, the siRNA knockdown of SNAI1 inhibited the HGF-mediated cellular migration (Fig. 3D). Collectively, these results indicate that SNAI1 is required to induce the HGF-mediated EMT in HCC cells.

In general, SNAI1 expression is regulated by ligand-receptor signal transduction through a downstream signal pathway that includes the Smad, MAPK, AKT, and GSK3 pathways (6, 22, 23). Sorafenib has been shown to inhibit RAF-MAPK signaling in HCC cells (24). Accordingly, we hypothesized that sorafenib might downregulate SNAI1 expression by inhibiting RAF-MAPK signaling, which is a unique activity of sorafenib. As

DOI:10.1158/1535-7163.MCT-10-0544

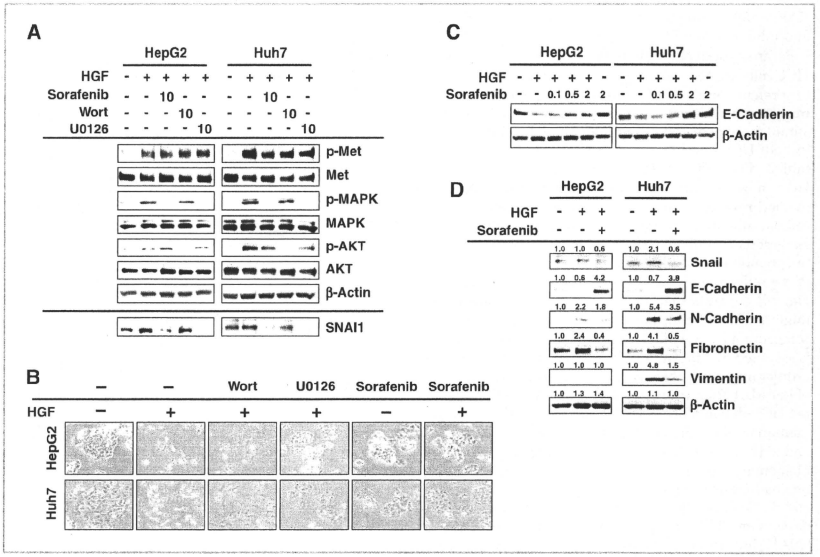

Figure 4. Sorafenib downregulates SNAI1 expression in HCC. A, as expected, sorafenib and the MEK inhibitor U0126 inhibited the HGF-mediated phosphorylation of MAPK, but the PI3K inhibitor wortmannin did not. Of note, SNAI1 expression was markedly downregulated by sorafenib and U0126. The HepG2 and Huh7 cells were exposed to 10 μmol/L of sorafenib or wortmannin or U0126 for 3 hours and were then stimulated with 10 ng/mL of HGF for 60 minutes. Wort, wortmannin. B, the HGF-mediated morphologic changes were canceled by sorafenib and U0126 but not by wortmannin in the HCC cells. The cells were exposed to sorafenib or wortmannin or U0126 for 48 hours with or without HGF (10 ng/mL) and then photographed. C, HGF-mediated downregulation of E-cadherin was canceled by sorafenib. The cells were stimulated with HGF (10 ng/mL) and treated with sorafenib at indicated concentration for 48 hours. D, HGF-mediated cadherin switching and upregulation of fibronectin and vimentin were canceled by sorafenib in the HCC cell lines. The cells were cultured with or without 2 μmol/L of sorafenib for 72 hours, with or without HGF (10 ng/mL), and then were analyzed using Western blot analysis. Densitometric data are shown above the Western blot.

expected, sorafenib and the MEK inhibitor U0126 (10 μmol/L) markedly inhibited the HGF-induced phosphorylation of MAPK, but the PI3K inhibitor wortmannin (10 μmol/L) did not. In contrast, only wortmannin inhibited the phosphorylation of AKT (Fig. 4A). Notably, SNAI1 expression was strongly downregulated by sorafenib and U0126 but not by wortmannin (Fig. 4A). These results showed that sorafenib downregulated SNAI1 expression via MAPK signaling. Meanwhile, we examined the HGF- and sorafenib-mediated expression changes of *SNAI2*, *ZEB1*, *ZEB2*, and *TWIST* using real-time RT-PCR and Western blot (Supplementary Fig. 3). Baseline and expression changes of SNAI2 and TWIST were very low compared with SNAI1, and the expression changes of ZEB1 and ZEB2 seemed not to be significant. Collectively, we considered that SNAI2, TWIST, ZEB1, and ZEB2 are not likely to be involved in the effect of HGF and sorafenib on EMT in this cell lines. Then, we examined the activity of sorafenib on HGF-mediated morphologic changes in HCC cells. HGF stimulation mediated the cell scattering and spindle-shaped changes, and these effects were clearly canceled by sorafenib and U0126, but not by wortmannin, in both HepG2 and Huh7 cells (Fig. 4B). These results were consistent with the results of Western blotting. To show whether sorafenib cancels the effect of HGF-mediated downregulation of E-cadherin, we examined the Western blot in dose–response analysis. Downregulation of E-cadherin was clearly canceled by sorafenib in a dose-dependent manner (Fig. 4C). Time-course analysis showed that HGF-mediated downregulation of E-cadherin was also canceled by sorafenib (Supplementary Fig. 4). HGF stimulation downregulated E-cadherin expression and upregulated N-cadherin, vimentin, and fibronectin in HCC cells; however, these effects were canceled by sorafenib in both HCC cell lines (Fig. 4D and Supplementary Fig. 2B). The mRNA data of N-cadherin in Huh7 cells were not correlated with protein level. These results show that sorafenib inhibits the

DOI:10.1158/1535-7163.MCT-10-0544

RAF-MAPK pathway, thereby downregulating SNAI1 and inhibiting the EMT in HCC.

Because sorafenib inhibits the HGF-mediated EMT in HCC cells, we next examined whether the inhibitory effect of sorafenib on the EMT leads to an inhibition of cellular migration in HCC cells. A scratch assay revealed that HGF stimulation increased cellular migration by about 2- fold in both HCC cell lines; however, sorafenib significantly inhibited this effect to the baseline levels (Fig. 5A). Similarly, a migration assay using the Boyden chamber method revealed that sorafenib canceled HGF-mediated cellular migration in both cell lines (Fig. 5B). These results suggest that sorafenib actually inhibits the cellular migrating phenotype of the EMT in HCC cells. The combination of migration data with siRNA and sorafenib (Fig. 3D and Fig. 5B) suggests that inhibitory effects of sorafenib on migration may be mediated by Snail downregulation in some tumors (e.g., Huh7) but not in others (e.g., HepG2). It is assumed that the inhibitory activity of sorafenib on the cellular migrating phenotype is due to its inhibitory effect of Raf-MAPK signaling pathway (Fig. 4A and B). Regarding HGF-dependent PI3K-AKT signaling pathway, wortmannin weakly inhibited the wound closure in Huh7 cells and to the same extent by sorafenib in HepG2 cells (Supplementary Fig. 5). In contrast, wortmannin has no effect on Snail levels or on HCC morphology changes (Fig. 4A and B). Collectively, we speculate that activation of HGF-dependent PI3K-AKT pathway may not be involved in SNAI1 induction or morphologic change but at least partially involved in cell migration independent of Raf-MAPK-SNAI1 signaling.

Taken together, these results indicate that sorafenib inhibits the HGF-mediated EMT, which is characterized by cadherin switching, morphologic changes, and an increase in the cellular migrating phenotype, by inhibiting Raf-MAPK signaling, resulting in the downregulation of SNAI1 in HCC cells (Fig. 6).

Discussion

Recent accumulating evidence has shown that the EMT is involved in drug sensitivity to several anticancer agents (25). Within this topic, the most intensively investigated drugs have been endothelial growth factor receptor (EGFR)–targeting drugs for the treatment of lung cancer. A clinical trial has revealed that lung cancer cells with strong E-cadherin expression exhibit a significantly longer time to progression after EGFR-TKI (tyrosine kinase inhibitor) treatment (26). Other studies on EGFR-targeting drugs have shown that mesenchymal type lung cancer cells exhibit an EMT-dependent acquisition of PDGFR, FGF receptor, and TGF-β receptor signaling pathways (27), and integrin-linked kinase is a novel target for overcoming HCC resistance to EGFR inhibition (28). Regarding sensitivity to gemcitabine, mesenchymal type cancer cells are reportedly associated with gemcitabine resistance in pancreatic cancer cells (29). The mechanism of resistance to gemcitabine has been shown

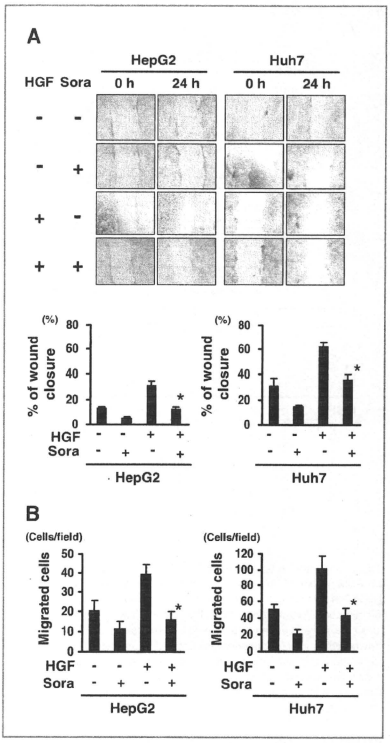

Figure 5. Sorafenib inhibits HGF-mediated cellular migration in HCC cells. A, a scratch assay revealed that HGF stimulation increased the cellular migration by about 2-fold, but sorafenib almost completely canceled the effect. The subconfluent HepG2 and Huh7 cells were scratched with a plastic pipette tip and incubated under the indicated conditions (control, 10 ng/mL of HGF; and HGF, 10 μmol/L of sorafenib). The scratch area was photographed and measured. The experiment was done in triplicate. *, sorafenib (–) versus (+), $P < 0.05$. B, migration assay using the Boyden chamber method revealed that sorafenib almost completely canceled the HGF-mediated cellular migration in both HCC cell lines. The cells were incubated under the indicated conditions: control, 10 ng/mL of HGF; and HGF, 10 μmol/L of sorafenib. *, sorafenib (–) versus (+), $P < 0.05$. Sora, sorafenib.

to involve the activation of Notch signaling, which is mechanistically linked with the mesenchymal chemoresistance phenotype of pancreatic cancer cells (30). Thus, baseline cellular characteristics based on the EMT phenotype might be useful not only as prognostic biomarkers for a malignant phenotype but also as predictive markers

DOI:10.1158/1535-7163.MCT-10-0544

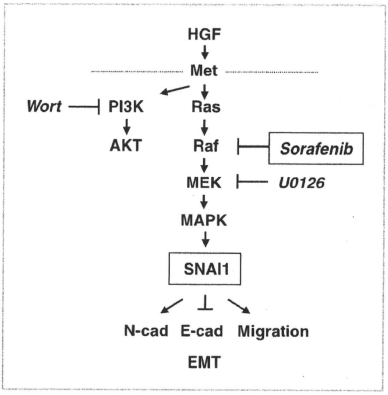

Figure 6. Diagram of the proposed mechanism by which sorafenib inhibits the EMT. Sorafenib inhibits the HGF-mediated EMT, which is characterized by morphologic changes, cadherin switching, and an increase in the cellular migrating phenotype. The anti-EMT effect of sorafenib occurs through the downregulation of SNAI1 by the inhibition of MAPK phosphorylation in HCC cells. Wort, wortmannin; N-cad, N-cadherin; E-cad, E-cadherin.

of sensitivity to anticancer agents. In this study, we focused on the signaling pathway responsible for inducing the EMT and showed that the multitarget TKI sorafenib downregulates SNAI1 by inhibiting Raf-MAPK signaling, thereby inhibiting the HGF-mediated EMT in HCC cells. Our findings may provide a novel insight into the actions of TKIs and their anti-EMT effects.

The mechanisms underlying the SNAI1-induced metastatic and aggressive phenotypes of cancer cells have recently been intensively investigated in both basic and clinical research studies. A novel aspect of the activity of SNAI1 is its involvement in immunosuppression. The SNAI1-induced EMT mediates regulatory T cells and impairs dendritic cells, accelerating cancer metastasis not only by enhancing invasion but also by inducing immunosuppression (31). A complex of histone deacetylase (HDAC) and SNAI1 plays an essential role in silencing E-cadherin (32), suggesting that the use of HDAC inhibitors to inhibit SNAI1 function might represent a promising therapeutic approach. On the other hand, large-scale clinical data on SNAI1 expression and the prognosis of patients with HCC were recently reported (33) and the overexpression of SNAI2 and/or TWIST was correlated with a worse prognosis. In contrast, no such significant differences were observed in samples that overexpressed SNAI2. The coexpression of Snail and TWIST was correlated with the worst prognosis for HCC (33). This evidence suggests that SNAI1 might be a useful therapeutic target for oncology. Our findings showed that sorafenib completely canceled the HGF-mediated SNAI1 induction in HepG2 and Huh7 cells. This activity of sorafenib, in addition to sorafenib's antiangiogenic effects, might contribute to a clinical benefit against metastatic and aggressive phenotypes in patients with HCC.

Disclosure of Potential Conflicts of Interest

No potential conflicts of interest were disclosed.

Acknowledgments

We thank Tomoko Kitayama and the staff of the Life Science Research Institute for their technical assistance.

Grant Support

This work was supported in part by the Third-Term Comprehensive 10-Year Strategy for Cancer Control and a Grant-in-Aid for Cancer Research (H20-20-9) from the Ministry of Health and Labor Scientific Research Grants.

The costs of publication of this article were defrayed in part by the payment of page charges. This article must therefore be hereby marked *advertisement* in accordance with 18 U.S.C. Section 1734 solely to indicate this fact.

Received June 9, 2010; revised October 25, 2010; accepted October 25, 2010; published online January 10, 2011

References

1. Jemal A, Murray T, Ward E, et al. Cancer statistics, 2005. CA Cancer J Clin 2005;55:10–30.
2. Yamamoto J, Kosuge T, Takayama T, et al. Recurrence of hepatocellular carcinoma after surgery. Br J Surg 1996;83:1219–22.
3. Wilhelm SM, Carter C, Tang L, et al. BAY 43-9006 exhibits broad spectrum oral antitumor activity and targets the RAF/MEK/ERK pathway and receptor tyrosine kinases involved in tumor progression and angiogenesis. Cancer Res 2004;64:7099–109.
4. Llovet JM, Ricci S, Mazzaferro V, et al.; SHARP Investigators Study Group. Sorafenib in advanced hepatocellular carcinoma. N Engl J Med 2008;359:378–90.
5. Cheng AL, Kang YK, Chen Z,, et al. Efficacy and safety of sorafenib in patients in the Asia-Pacific region with advanced hepatocellular carcinoma: a phase III randomised, double-blind, placebo-controlled trial. Lancet Oncol 2009;10:25–34.
6. Peinado H, Olmeda D, Cano A. Snail, Zeb and bHLH factors in tumour progression: an alliance against the epithelial phenotype?Nat Rev Cancer 2007;7:415–28.
7. Hugo H, Ackland ML, Blick T, et al. Epithelial-mesenchymal and mesenchymal-epithelial transitions in carcinoma progression. J Cell Physiol 2007;213:374–83.
8. Tsuji T, Ibaragi S, Hu GF. Epithelial-mesenchymal transition and cell cooperativity in metastasis. Cancer Res 2009;69:7135–9.
9. Gentile A, Trusolino L, Comoglio PM. The Met tyrosine kinase receptor in development and cancer. Cancer Metastasis Rev 2008;27:85–94.
10. Eder JP, Vande Woude GF, Boerner SA, LoRusso PM. Novel therapeutic inhibitors of the c-Met signaling pathway in cancer. Clin Cancer Res 2009;15:2207–14.
11. Yang H, Magilnick N, Noureddin M, Mato JM, Lu SC. Effect of hepatocyte growth factor on methionine adenosyltransferase genes

DOI:10.1158/1535-7163.MCT-10-0544

and growth is cell density-dependent in HepG2 cells. J Cell Physiol 2007;210:766–73.
12. Mizuguchi T, Nagayama M, Meguro M, et al. Prognostic impact of surgical complications and preoperative serum hepatocyte growth factor in hepatocellular carcinoma patients after initial hepatectomy. J Gastrointest Surg 2009;13:325–33.
13. Chau GY, Lui WY, Chi CW, et al. Significance of serum hepatocyte growth factor levels in patients with hepatocellular carcinoma undergoing hepatic resection. Eur J Surg Oncol 2008;34:333–8.
14. Yamagamim H, Moriyama M, Matsumura H, et al. Serum concentrations of human hepatocyte growth factor is a useful indicator for predicting the occurrence of hepatocellular carcinomas in C-viral chronic liver diseases. Cancer 2002;95:824–34.
15. Tanaka K, Arao T, Maegawa M, et al. SRPX2 is overexpressed in gastric cancer and promotes cellular migration and adhesion. Int J Cancer 2009;124:1072–80.
16. Matsumoto K, Arao T, Tanaka K, et al. mTOR signal and hypoxia-inducible factor-1 alpha regulate CD133 expression in cancer cells. Cancer Res 2009;69:7160–4.
17. Kaneda H, Arao T, Tanaka K, et al. FOXQ1 is overexpressed in colorectal cancer and enhances tumorigenicity and tumor growth. Cancer Res 2010;70:2053–63.
18. Lee JM, Dedhar S, Kalluri R, Thompson EW: The epithelial-mesenchymal transition: new insights in signaling, development, and disease. J Cell Biol 2006;172:973–81.
19. Wheelock MJ, Shintani Y, Maeda M, Fukumoto Y, Johnson KR. Cadherin switching. J Cell Sci 2008;121:727–35.
20. Lo HW, Hsu SC, Xia W, et al. Epidermal growth factor receptor cooperates with signal transducer and activator of transcription 3 to induce epithelial-mesenchymal transition in cancer cells via up-regulation of TWIST gene expression. Cancer Res 2007;67:9066–76.
21. Vincent T, Neve EP, Johnson JR, et al. A SNAIL1-SMAD3/4 transcriptional repressor complex promotes TGF-beta mediated epithelial-mesenchymal transition. Nat Cell Biol 2009;11:943–50.
22. Larue L, Bellacosa A. Epithelial-mesenchymal transition in development and cancer: role of phosphatidylinositol 3' kinase/AKT pathways. Oncogene 2005;24:7443–54.
23. Zavadil J, Böttinger EP. TGF-beta and epithelial-to-mesenchymal transitions. Oncogene 2005;24:5764–74.
24. Liu L, Cao Y, Chen C, et al. Sorafenib blocks the RAF/MEK/ERK pathway, inhibits tumor angiogenesis, and induces tumor cell apoptosis in hepatocellular carcinoma model PLC/PRF/5. Cancer Res 2006;66:11851–8.
25. Voulgari A, Pintzas A. Epithelial-mesenchymal transition in cancer metastasis: mechanisms, markers and strategies to overcome drug resistance in the clinic. Biochim Biophys Acta 2009;1796:75–90.
26. Yauch RL, Januario T, Eberhard DA, et al. Epithelial versus mesenchymal phenotype determines *in vitro* sensitivity and predicts clinical activity of erlotinib in lung cancer patients. Clin Cancer Res 2005; 11:8686–98.
27. Thomson S, Petti F, Sujka-Kwok I, Epstein D, Haley JD. Kinase switching in mesenchymal-like non-small cell lung cancer lines contributes to EGFR inhibitor resistance through pathway redundancy. Clin Exp Metastasis 2008;25:843–54.
28. Fuchs BC, Fujii T, Dorfman JD, et al. Epithelial-to-mesenchymal transition and integrin-linked kinase mediate sensitivity to epidermal growth factor receptor inhibition in human hepatoma cells. Cancer Res 2008;68:2391–9.
29. Arumugam T, Ramachandran V, Fournier KF, et al. Epithelial to mesenchymal transition contributes to drug resistance in pancreatic cancer. Cancer Res 2009;69:5820–8.
30. Wang Z, Li Y, Kong D, et al. Acquisition of epithelial-mesenchymal transition phenotype of gemcitabine-resistant pancreatic cancer cells is linked with activation of the notch signaling pathway. Cancer Res 2009;69:2400–7.
31. Kudo-Saito C, Shirako H, Takeuchi T, Kawakami Y. Cancer metastasis is accelerated through immunosuppression during Snail-induced EMT of cancer cells. Cancer Cell 2009;15:195–206.
32. von Burstin J, Eser S, Paul MC, et al. E-cadherin regulates metastasis of pancreatic cancer *in vivo* and is suppressed by a SNAIL/HDAC1/HDAC2 repressor complex. Gastroenterology 2009;137:361–71.
33. Yang MH, Chen CL, Chau GY, et al. Comprehensive analysis of the independent effect of Twist and Snail in promoting metastasis of hepatocellular carcinoma. Hepatology 2009;50:1464–74.

Cancer Science
The official journal of the Japanese Cancer Association

Enhanced expression of nuclear factor I/B in oxaliplatin-resistant human cancer cell lines

Eiji Kashiwagi,[1,2] Hiroto Izumi,[1] Yoshihiro Yasuniwa,[1] Ryoko Baba,[3] Yoshiaki Doi,[3] Akihiko Kidani,[1] Tokuzo Arao,[4] Kazuto Nishio,[4] Seiji Naito[2] and Kimitoshi Kohno[1,5]

[1]Department of Molecular Biology, School of Medicine, University of Occupational and Environmental Health, Kitakyushu; [2]Department of Urology, Graduate School of Medical Sciences, Kyushu University, Fukuoka; [3]Department of Anatomy, School of Medicine, University of Occupational and Environmental Health, Kitakyushu; [4]Department of Genome Biology, Kinki University School of Medicine, Osaka, Japan

(Received September 17, 2010/Revised October 13, 2010/Accepted October 17, 2010/Accepted manuscript online October 26, 2010/Article first published online November 19, 2010)

Oxaliplatin is a third-generation platinum drug that has favorable activity in cisplatin-resistant cells. However, the molecular mechanisms underlying oxaliplatin resistance are not well understood. To investigate the molecular mechanisms involved, resistant cell lines were independently derived from colon cancer (DLD1) and bladder cancer (T24) cells. Oxaliplatin-resistant DLD1 OX1 and DLD1 OX2 cell lines were approximately 16.3-fold and 17.8-fold more resistant to oxaliplatin than the parent cell lines, respectively, and had 1.7- and 2.2-fold higher cross-resistance to cisplatin, respectively. Oxaliplatin-resistant T24 OX2 and T24 OX3 cell lines were approximately 5.0-fold more resistant to oxaliplatin than the parent cell line and had 1.9-fold higher cross-resistance to cisplatin. One hundred and fifty-eight genes commonly upregulated in both DLD1 OX1 and DLD1 OX2 were identified by microarray analysis. These genes were mainly involved in the function of transcriptional regulators (14.6%), metabolic molecules (14.6%), and transporters (9.5%). Of these, nuclear factor I/B (NFIB) was upregulated in all oxaliplatin-resistant cells. Downregulation of NFIB rendered cells sensitive to oxaliplatin, but not to cisplatin. Forced expression of NFIB induced resistance to oxaliplatin, but not to cisplatin. Taken together, these results suggest that NFIB is a novel and specific biomarker for oxaliplatin resistance in human cancers. (*Cancer Sci* 2011; 102: 382–386)

One of the major obstacles in cancer chemotherapy is intrinsic and/or acquired resistance, which mainly involves pleiotropic mechanisms. We have extensively investigated the molecular mechanisms underlying cisplatin resistance, and found alterations in various cellular processes such as drug transport, drug accumulation, drug detoxification, DNA repair, transcription, and apoptosis.[1–3] Oxaliplatin is a platinum-containing anticancer agent with activity against cisplatin-resistant cell lines.[4,5] Oxaliplatin possesses a differential spectrum of activity compared with cisplatin[6–9] and is effective in patients with colon cancer and other tumors, such as ovarian cancers.[10,11] Studies on oxaliplatin resistance started several years ago[12–18] and suggest a similar mechanism to that seen for cisplatin resistance.[8] Oxaliplatin and cisplatin kill cancer cells by forming DNA adducts that inhibit DNA replication and transcription.[6] However, studies investigating the *in vitro* cytotoxic activity against cancer cells suggest that oxaliplatin and cisplatin have different sensitivity profiles, indicating potential differences in the molecular mechanisms involved in drug resistance.[19,20] We have developed and characterized oxaliplatin-resistant human cancer cell lines to further understand the mechanisms involved in oxaliplatin resistance. In this study, we investigated a novel candidate gene that is specifically associated with acquired oxaliplatin resistance.

Materials and Methods

Cell culture and establishment of oxaliplatin-resistant cell lines. The human colon cancer cell line, DLD1, was cultured in RPMI. The oxaliplatin-resistant cell lines, DLD1 OX1 and DLD1 OX2, were derived from DLD1 cells. All cell lines were maintained in a 5% CO_2 atmosphere at 37°C. Human epidermoid cancer cells (HeLa), prostate cancer cells (PC3), and bladder cancer cells (T24) were cultured in Eagle's minimal essential medium. All media were purchased from Nissui Seiyaku (Tokyo, Japan) and contained 10% FBS. The cisplatin-resistant H/CP4 and P/CDP6 cell lines were derived from HeLa and PC3 cells, respectively, as previously described,[21] and were maintained in medium supplemented with 10 μM cisplatin. Oxaliplatin-resistant cell lines (DLD1 OX1 and OX2; T24 OX2 and OX3) were established from DLD1 and T24 cells, respectively, by stepwise, continuous treatment with oxaliplatin. Cell lines were then maintained in medium supplemented with 5 μM oxaliplatin.

Antibodies and drugs. Anti-nuclear factor I/B (NFIB) (39091), anti-Tip60 (sc-5275), and anti-hemagglutinin (HA)-peroxidase (3F10) were purchased from Active Motif (Carlsbad, CA, USA), Santa Cruz Biotechnology (Santa Cruz, CA, USA), and Calbiochem (Darmstadt, Germany), respectively. Cisplatin was purchased from Sigma (St. Louis, MO, USA). Oxaliplatin was a kind gift from Yakult (Tokyo, Japan).

Plasmid construction and establishment of stable transfectants. To prepare the HA-tagged NFIB expression plasmid, cDNA derived from HeLa cells was amplified using the primer pair 5′-ATGATGTATTCTCCCATCTGTCTC-3′ and 5′-CTAGCCCAGGTACCAGGACTGG-3′. The PCR products fused with the ATGGGTTATCCGTATGATGTTCCTGATTATGCT sequence expressing the HA amino acid (YPYDVPDYA) at the N-terminus was ligated into a pcDNA3.1/Hygro(+) vector (Invitrogen, Carlsbad, CA, USA). To prepare the HA-NFIB stable transfectants, DLD1 cells were transfected with pcDNA3.1/Hygro(+)-HA-NFIB and cultured with 500 ng/mL hygromycin. After 3 weeks, single colonies were isolated and cultured with hygromycin. Transfectants stably expressing HA-NFIB (HA-NFIB CL1 and CL3), were then used in MTT assays.

Knockdown using siRNA. The following double-stranded RNA 25-bp oligonucleotides were commercially generated (Invitrogen): *NFIB* siRNA: *siNFIB #1*, 5′-GCUGGAAGUCGAACAUGGCACGAAA-3′ (sense) and 5′-UUUCGUGCCAUGUUCGACUUCCAGC-3′ (antisense); *siNFIB #2*, 5′-GGAGUUGCACACAGUGUCAUCUCAA-3′ (sense) and 5′-UUGAGAUGACACUGUGUGCAACUCC-3′ (antisense). siRNAs (200 pmol) were mixed with 5 μL Lipofectamine 2000 (Qiagen, Hilden, Germany) according to the manufacturer's instructions.

[5]To whom correspondence should be addressed.
E-mail: k-kohno@med.uoeh-u.ac.jp

doi: 10.1111/j.1349-7006.2010.01784.x

After 20 min, 5×10^5 cancer cells were gently added, mixed, and incubated for a further 20 min. Transfected cells were used for Western blotting and colony formation assays.

Oligonucleotide microarray studies and microarray analysis. The microarray procedure was carried out as previously described.[21] In brief, total RNA extracts were collected from DLD1, DLD1 OX1, and DLD1 OX2 cells. Eight GeneChips (Affymetrix, Santa Clara, CA, USA) were used for analysis. The microarray analysis was carried out using the BRB Array Tools software version 3.3.0 (http://linus.nci.nih.gov/BRB-ArrayTools.html) developed by Dr Richard Simon and Amy Peng.

Cytotoxicity analysis by colony formation and water-soluble tetrazolium salt (WST)-8 assays. For the WST-8 assay, 1.0×10^3 cells were seeded into 96-well plates. The following day, the indicated concentrations of oxaliplatin and cisplatin were applied. After 72 h, surviving cells were stained with TetraColor ONE (Seikagaku, Tokyo, Japan) for 180 min at 37°C according to the manufacturer's instructions. The absorbance was then measured at 450 nm. For the colony-formation assay, 300 PC3 or DLD1 OX1 cells were seeded into 35-mm dishes with 2 mL culture medium. The following day, cells were treated with the indicated concentrations of oxaliplatin or cisplatin. After 7 days, the number of colonies was counted. Each count, or colony number, in the absence of drug corresponded to 100%. The IC50 values were calculated from the concentration–response curve.

Western blot analysis. To prepare the nuclear extracts we used buffer-A, containing 10 mM Hepes-KOH (pH 7.9), 10 mM KCl, 0.1 mM EDTA-NaOH (pH 8.0), 0.1 mM EGTA, 1 mM DTT, and 0.5 mM PMSF, and buffer-Y, containing 50 mM Tris–HCl (pH 8.0), 1 mM EDTA, 120 mM NaCl, 0.5% Nonidet P-40, and 0.5 mM PMSF. Briefly, cells were suspended in buffer-A and incubated on ice for 15 min. After addition of Nonidet P-40 (0.3% final concentration), cells were centrifuged at 2000*g* for 5 min. Pellets (nuclear material) were sonicated for 20 s with buffer-Y. To prepare whole cell lysates, cells were sonicated for 20 s with buffer-Y. Whole-cell lysates (50 μg) or nuclear extracts (100 μg) were separated by SDS-PAGE and transferred onto PVDF membranes membranes. Western blot analysis was carried out using appropriately diluted antibodies, and the membrane was developed using a chemiluminescence protocol (GE Healthcare, Waukesha, WI, USA). Images were obtained using an image analyzer (LAS-4000 mini; Fujifilm, Tokyo, Japan).

Statistical analysis. Student's *t*-test was used for statistical analysis of the variables between two groups. All error bars indicate standard deviation. A *P*-value >0.05 was considered significant.

Results

Drug sensitivity profiles of parental and resistant cell lines. Electron microscopic study of the oxaliplatin-resistant cell lines revealed similar morphology to that of the parental lines (data not shown) and the growth rate of the resistant cells was similar to that of the parental cells (data not shown). The drug sensitivity profiles of the oxaliplatin-resistant cells determined using the WST-8 assay are shown in Figure 1(A). DLD1 OX1 and DLD1 OX2 were approximately 16.3-fold and 17.8-fold more resistant to oxaliplatin than the parental cell lines and showed 1.7-fold and 2.2-fold higher cross-resistance to cisplatin, respectively. The oxaliplatin-resistant bladder cancer lines (T24 OX2 and T24 OX3) showed an approximate 5.0-fold increase in relative resistance with 1.9-fold higher cross-resistance to cisplatin. As shown in Figure 1(B), the two cisplatin-resistant cell lines also showed weak cross-resistance to oxaliplatin.

DNA microarray analysis of oxaliplatin-resistant cells. We analyzed the gene expression profiles DLD1 OX1 and DLD1 OX2 cells and found that the expression levels of 158 genes were increased more than 3.0-fold compared with the parental lines (Table S1). Of these 158 genes, 23 (approximately 15%) were involved in transcriptional regulation. Twenty-three genes were categorized as metabolic molecules and 15 as transporters. Approximately 34% of the upregulated genes were unclassified (Fig. 2).

Overexpression of NFIB in oxaliplatin-resistant cells. We previously showed that various transcription factors are overexpressed in drug-resistant cells.[21–25] Therefore, we focused our attention on the expression of transcription factors. The transcription factor, NFIB, was overexpressed in the two oxaliplatin-resistant colon cancer cell lines and the two oxaliplatin-resistant bladder cancer cell lines (Fig. 3A). However, subtle expression was also observed in the parental DLD1 and T24 cells. The NFIB is only localized in nuclei of both parental and oxaliplatin-resistant cells (data not shown). To confirm overexpression of the *NFIB* gene, oxaliplatin-resistant cells were transfected with two NFIB-specific siRNAs (Fig. 3B). We also found that human prostate cancer (PC3) cells expressed NFIB.

Specific involvement of NFIB in oxaliplatin resistance. Next, we silenced NFIB expression in PC3 and DLD1 OX1 cells and carried out colony formation assays. Knockdown of NFIB expression sensitized the cells to oxaliplatin, but not to cisplatin (Fig. 4). To confirm these results, we established two cell lines overexpressing NFIB from DLD1 cells and evaluated their drug sensitivity (Fig. 5A). The upper band in the figure corresponds to the HA-tagged NFIB product derived from the expression plasmid, and the lower band to endogenous NFIB. As shown in Figure 5(B), both cell lines overexpressing NFIB were resistant to oxaliplatin, but not to cisplatin.

Discussion

Both intrinsic and acquired drug resistance hinder the treatment of solid tumors. Anticancer agents can activate a variety of signal transduction pathways, and trigger genome-wide responses. The isolation of drug-resistant cell lines is a well-established strategy for analyzing the biochemical changes underlying drug resistance. Cisplatin is a potent anticancer agent used for the treatment of various solid tumors; oxaliplatin is active against solid tumors that are cisplatin-sensitive, or have intrinsic or acquired cisplatin resistance.[4,5] This difference in activity indicates that these platinum-containing agents might have different modes of action, resulting in different levels of sensitivity to cisplatin and oxaliplatin. Oxaliplatin is used to treat patients with colon cancer in combination with 5-fluorouracil or irinotecan.[26] In this study, we established oxaliplatin-resistant cell lines from human colon and bladder cancer cells to identify the factors that make cells resistant to chemotherapy, enabling them to survive and develop further resistance. Oxaliplatin-resistant cells show both similar and different mechanisms to cisplatin-resistant cells. The transcription factors circadian locomotor output cycles kaput (Clock), activating transcription factor 4 (ATF4), and Y box binding protein 1 (YB-1) were upregulated in both oxaliplatin-resistant and cisplatin-resistant cells (data not shown). These results may explain the cross-resistance to cisplatin shown by our oxaliplatin-resistant cells. The expression of excision repair cross-complementing rodent repair deficiency, complementation group 1 (ERCC1), was often upregulated in cisplatin-resistant cells and is a good predictive marker for the efficacy of cisplatin-based chemotherapy.[27,28] However, we did not observe upregulation of ERCC1 expression in oxaliplatin-resistant cells (data not shown). Extensive analysis of oxaliplatin-resistant cells and further understanding of the molecular mechanisms of drug resistance are important to overcome drug resistance and improve platinum-based cancer chemotherapy. Many genes are expected to be differentially expressed in any given pair of cell lines, whether sensitive or resistant to oxaliplatin. The goal is to identify the set of genes